Significance of Tumor Mutation Burden Related Immune Gene in the Progression and Prognosis of Clear Cell Renal Cell Carcinoma

Zhirong Yang
The Fujian Pinghe County People's Hospital
Duo Yun
Inner Mongolia Yuanhe Mongolian Medicine Research Institute, Inner Mongolia Yuanhe Mongolian Medicine Research Institute
Longmei Dai
Sanming No.2 Hospital
Qinqin Wang
The Affiliated Nanping First Hospital of Fujian Medical University
Xiangli Guo
Fujian Medical University affiliated Zhangzhou Hospital
Wang JinYong
Affiliated Longyan First Hospital of Fujian Medical University
Yang Su
The First Affiliated Hospital of Anhui Medical University
Yaofeng Yun (yyfmzyy@163.com)
Hohhot Mongolian Medicine and Chinese Traditional Medicine Hospital
Zhifei Che
Renmin Hospital of Wuhan University

Research Article

Keywords: clear cell renal cell carcinoma, immunotherapy, tumor mutation burden, bioinformatics analysis

Posted Date: June 1st, 2021

DOI: https://doi.org/10.21203/rs.3.rs-504368/v1

Abstract

Background: Clear cell renal cell carcinoma (ccRCC) is a common renal malignant disease with a poor prognosis. There were limited studies focus on the relationship between Tumor mutation burden (TMB) and ccRCC.

Methods: Based on TCGA-ccRCC cohort, we summarized the status of gene mutations in ccRCC. Then, we analyzed the relationship between TMB and clinical characteristic. Meanwhile, we identified some TMB-related immune genes through the intersection of TMB-Related differentially expressed genes (DEGs) and immune related genes. Finally, we selected the highest correction and novel genes for the future analysis.

Results: The most common mutation of Variant Classification, Variant Type, SNV Class were missense mutations, SNP, C>T, respectively. Higher TMB related to shorter overall survival (OS), lower age and grade. Finally, we identified PAEP gene, a novel TMB-related immune gene in ccRCC, which was significantly overexpression in ccRCC tissues and cells with progression and poor survival in ccRCC patients. Furthermore, PAEP promoted the invasion, migration, and proliferation of ccRCC cells. Mechanistically, PAEP suppressed the PI3K/Akt/NF-κB signaling pathway.

Conclusion: Our study suggests that PAEP might represents a potential target of antibody immunotherapy for ccRCC patients.

Introduction

Renal cell carcinoma (RCC) is the most common genitourinary malignancy. As the most common type of RCC, Clear cell renal cell carcinoma (ccRCC) accounts for 75~80% of all RCC cases [1-3]. Recently, surgery and targeted therapy are the most common and effective clinical treatments for ccRCC patients. However, its overall mortality rates are still slightly increased[2], partly due to early-stage metastasis of the disease. Therefore, some novel markers for early diagnostic and therapeutic targets involved in ccRCC progression are urgently required with significant clinical value. In recent years, antibody immunotherapy represents a promising therapy for the clinical treatment of ccRCC patents, successfully developed and widely applied. For example, Immune checkpoint inhibitors (ICI) such as PD-1/PD-L1 inhibitors develop as a potential clinical strategy for ccRCC[4, 5]. However, ccRCC patients sometimes show low objective response rates against ICI. Tumor mutation burden (TMB) is defined as a total number of somatic coding mutations in the exon coding region of the genome of a tumor cell. TMB is a potential biomarker for predicting ICI response in varying tumors[6]. High TMB patients with high TMB tended to get better treatment efficacy against PD-1/PD-L1 inhibitors [7, 8]. The connection between TMB and immune infiltration was deviated from varied tumors. Nevertheless, limited studies on TMB-related immune genes in ccRCC, so we tried to research the potential relationship between TMB and ccRCC. Finally, we select a novel of TMB-related immune gene for the further analysis.

Methods

Data source and mutation analysis

The data of ccRCC patients, including “mask somatic mutation”, transcriptome profiles and clinical data, was obtained from the TCGA database on November 08,2020. At the same time, we used the Mutect algorithm to processed “mask somatic mutation” data and visualized the results using the “maftoools” R package. Then, we categorized the ccRCC patients into high-TMB group and low-TMB group according to the median value of TMB. To analyze the correlation between TMB status and several clinicopathological characteristics, we analyzed the significance. We also analyzed the difference of overall survival (OS) between the high-TMB group and low-TMB group using Kaplan-Meier statistics. To evaluate the diagnostic value of TMB-related immune genes in ccRCC, we performed Receiver Operating Characteristic (ROC) curves and calculated the area under the ROC curve (AUC) to assess the diagnostic efficiency.

TMB-Related differentially expressed genes and functional enrichment analysis

To understand the TMB-Related function, we used the R package “limma v3.38.3” to perform TMB-Related differentially expressed genes (DEGs) between the above two TMB subgroup with $p < 0.05$ and $|logFC| > 1.0$. Meanwhile, we visualized the DEGs with volcanic plot and heatmap. Nevertheless, Gene Ontology (GO) categories and Kyoto Encyclopedia of Genes and Genomes (KEGG) were identified using R package “clusterProfiler, org.Hs.eg.db, enrichplot” to identify the functional enrichment and pathway enrichment of all DEGs[9]. All above results were visualized by R package “ggplot2, heatmap, ggpubr, ggthemes”.

Identification and Co-expression analysis of TMB-related immune genes

On the other hand, we obtained a list of immune related genes (IRG) from the Immport data (https://www.immport.org), then we defined the common genes as TMB-related immune genes between immune related genes and DEGs using R package “**ggplot2**”. Finally, we performed the expression, correlation , and risk score distribution, survival status of the TMB-related immune genes among patients based on the expression of these genes using R package “corrplot, ggplot2, heapmap”. Finally, we selected the highest correction and novel gene for the future analysis, including expression analysis, Gene Set Enrichment Analysis (GSEA), OS, ROC and clinical correlation with GSEA project (4.0.3) and R package “pROC, ggplot2, CBCgrps”[10, 11].

Cell culture and transfection

The human ccRCC cell line,769-P, 786-0, A498 and ACHN, was purchased from ASY Biotechnology Ltd., Corp (Wuhan, China). All the cells were cultured in RPMI-1640 medium containing 10% fetal bovine serum (FBS). Cells were maintained at 37 °C and incubated with 5% CO_2.The plasmids were supplied by GeneChem Corp (Shanghai, China). Transfection conditions were reference to our previous paper. Briefly,

the shRNA target sequence was shPAEP1, 5'-AAGATCAACTATACGGTGG-3', shPAEP2, 5'-AAGAGCCGTGCCGTTTCTA-3'. Conforming to the manufacturer's guidance, the 786-0 cells were transfected with shRNA non-sense control (shRNA-Con group) or with PAEP shRNA (shRNA-PAEP group) using lentiviral particles at a MOI (100:1) of 100 pfu/cell in the presence of polybrene. In order to acquire PAEP knockdown cell lines, the transfected cells were treated with 5 mg/mL of puromycin. Then, the resistant colonies were collected and cultivated for further analyses.

Patient selection and preparation of tissue

36 patients who were diagnosed as ccRCC at Renmin Hospital of Wuhan University were enrolled in our study (approval no. 2017K-C015). More detailed information of the patents is previous described[1] . The ccRCC and their paired-normal tissues were snap-frozen immediately after removal and stored at −80°C. All experiments were carried out in accordance with the Code of Ethics of the World Medical Association, and the study was approved by the ethics committee of Renmin Hospital of Wuhan University (approval no. 2017K-C015). All the human subjects gave their informed consent for the use of their samples and data.

Gene expression analysis

Lysates from ccRCC cells were electrophoresed on 10% SDS-PAGE, then transferred to PVDF membranes (Millipore, Billerica, MA), as previously described. Briefly, the membranes blocked with skim milk at room temperature for 1h, then incubated with anti-β-Actin or anti-PAEP (Proteintech,21099-1-AP, USA) at 4 °C overnight. The membranes were washed with TBST three times and then incubated in HRP-conjugated secondary antibodies. β-Actin acted as an internal control. According to the manufacturer's instructions, total RNA from the ccRCC and their paired-normal tissues was extracted using the Trizol reagent. The concentration of the RNA was determined using ultraviolet spectrophotometry. The cDNA was synthesized using a PrimeScript RT Reagent Kit with gDNA Eraser. Quantitative real-time PCR analysis for PAEP mRNA levels was performed using a SYBR Premix Ex Taq II through an Applied Biosystems 7500 Real-Time PCR System. Relative mRNA expression levels were calculated using the relative Ct method, and the fold change compared with β-actin as the control. The primer sequences were referred to previous papers, as follows: Forward (PAEP):**5-CCTGTTTCTCTGCCTACAGGA-3**, Reverse (PAEP):**5-CCTGTTTCTCTGCCTACAGGA-3**; Forward (β-Actin):5-GTCCACCGCAAATGCTTCTA-3, Reverse (β-Actin):5-TGCTGTCACCTTCACCGTTC-3.

Cell proliferation assay, migration and invasion assays

The CCK-8 kit (cat. no. CK04, Dojindo, Japan) was used to analyze cell proliferation. Briefly, according to the manufacturer's instructions, 3000 cells in each well were cultured in a 96-well plate to investigate the effect of PAEP knockdown on cell proliferation. A multilabel counter (Perkin Elmer, Singapore) was used to calculate cells number by measuring the OD450. 24-well Transwell plates (cat. no. 3422, Corning, USA) with or without Matrigel matrix (cat. no. 356234, BD Biosciences, USA) were used for migration assay and invasion assay. The upper chambers and the lower chambers were seeded 1×10^5 cells in 200 μl without

FBS RPMI 1640 medium and added 600 μ l of RPMI 1640 containing 20% FBS, respectively. Subsequently, cells that migrated or invaded through the bottom of chambers were fixed with 4% paraformaldehyde, and then stained with 0.05% crystal violet for 30 min, as previously described [12]. Finally, a microscope counted the number of migration or invasion cells. For the colony formation assay, the cells were seeded and cultivated into 6-well plates with 500 cells per well. Then, the cells were fixed in 75% alcohol for 30 min and stained with 0.05% crystal violet for 30 min after 14 days. All above experiments were performed with three times and calculated mean using the ImageJ software.

Statistical analysis

We selected the **TMB-Related** DEGs with $p < 0.05$ and $|logFC| > 1.0$ to further assess. Statistical analysis was performed with R project 3.6.0. The KM analysis and log-rank test were used to assess OS in the ccRCC cohort. The Chi-square test were used to assess correlation between PAEP expression and clinicopathologic characteristics of ccRCC patients. Two-tailed t -tests and one-way analysis of variance (ANOVA) were used to analyze cell culture experiments. *P* value <0.05 was considered as statistically significant.

Results

Mutation analysis

Somatic mutation profiles of **537** ccRCC patients downloaded from TCGA database were analyzed and visualized using R package “maftools”[13]. A waterfall plot was performed to exhibit the detailed mutation information in each sample. The majority of Variant Classification, Variant Type, SNV Class were missense mutations, SNP, C>T, respectively (**Figure 1a i-iii**). Counting each sample separately, the median and maximum of mutations in the TCGA-ccRCC cohort were 47 and 1611, respectively (**Figure 1a iv, Figure 1b**). In addition, we exhibited the number of each variant classification in the different sample using box plots **(Figure.1a v)**. The top 10 mutated genes in the 336 ccRCC patients were VHL (49%), PBRM1 (42%), TTN (18%), SETD2 (12%), BAP1 (10%), MUC16 (7%), MTOR (7%), KDM5C (6%), HMCN1 (5%), DNAH9 (5%) **(Figure 1**a **vi, Figure 1b, Figure 1d**), while the PBRM1 and VHL have the highest correlation **(Figure 1c)**.

Correlation of TMB with prognosis and clinical features

After the clinical data of ccRCC patients were collected from TCGA, we selected **336** patients with complete information. Based on the median TMB value (**1.29)**, we divided 336 patients into high-and low-TMB groups (n=163 VS n=173). As showed in the KM curve, the high-TMB group had significantly poor OS outcomes (P=0.007) (**Figure 2h**). Besides, the correlation of TMB with clinical features showed that only age and grade were significantly associated with TMB (p<0.05) (**Figure 2a, f**), the other clinical characteristics showed no significantly difference (**Figure 2b, c, d, e, g**).

TMB-Related differentially expressed genes and Functional enrichment analysis

According to the DEGs expression analysis between high-TMB group and low-TMB group, a total of **120** DEGs with $|\log_2 FC| > 1$ and FDR < 0.05 was identified. There are **44** up-regulated genes and **76** down-regulated genes in the high-TMB group, compared to the low-TMB group. The heatmap and volcano plot showed the top **40** DEGs ranked in the order of FDR and all DEGs, respectively (**Figure3a, b**). According to GO and KEGG analysis, DEGs were enriched in the function enrichment of apical part of cell, apical plasma membrane, axon terminus and the pathway of Calcium signaling pathway, Vibrio cholerae infection and Taurine and hypotaurine metabolism (**Figure 3c, d**).

Comparison of gene expression profiles between two tmb groups

We further identified the TMB-related immune genes through the intersection of **1793** immune related genes and **120** DEGs for subsequent analysis (**Figure 4a**). Then, we selected 8 TMB-related immune genes including CRP, IGHA2, IGLC3, IL6, LBP, LCN1, PAEP, SLIT2. We extracted the mRNA expression of each TMB-related immune genes to draw the box plot, heatmap and correlation heatmap (**Figure 4b, c, d**). The results revealed that IGHA2, IGLC3, PAEP were increased, while CRP, LCN1 and SLIT2 decreased, IL6 and LBP resting in ccRCC tissues, compared to the normal tissues (**Figure 4b, c**). Importantly, PAEP and LCN1 had the highest correlation score (0.96) (**Figure 4d**).in addition, the ccRCC patents with higher risk scores, composing by these genes, had poor outcomes (**Figure 4e**). Finally, we selected the PAEP which is a never reported gene in ccRCC for the further research.

PAEP was overexpression and associated with shorter survival in ccRCC patents

Considering PAEP overexpression in ccRCC, we further investigated whether it contributed to ccRCC progression. Thus, we chose the 786-0 cells which had the highest levels of PAEP for further investigation (**Figure 5a, b**). 786-0 cells were transfected with short hairpin RNAs (shRNAs) targeting to PAEP, which significantly silenced the PAEP expression (**Figure7a**). PAEP was significantly overexpressed in the TCGA-ccRCC cohort, compared to the normal group (**Figure 5f**), which was further validated in ccRCC cells and ccRCC tissues by Western blot analysis and RT-qPCR (**Figure 5c-e**). Moreover, analysis of clinical characteristics indicated that PAEP overexpression was significantly correlated with Primary tumor size, TNM stage and Fuhrman grade (**Table 1**). Importantly, Kaplan-Meier analysis revealed that ccRCC patients with high PAEP expression had poor OS and DFS in the TCGA cohorts and further confirmed in our cohort (without DFS result) (**Figure5g-i**), indicating that PAEP upregulation was potentially related to the ccRCC progression. To evaluate the diagnostic value of PAEP in ccRCC, we constructed ROC curve and calculated the AUC (**Figure5j**). The ROC curve of PAEP indicated it was a medium diagnostic tool with an AUC is 0.764. We performed GSEA to reveal potential molecular mechanism of PAEP regulating the progression of ccRCC. The results showed that all the significant pathways were enrichment in the PAEP overexpression group related to various tumorigenesis-related characteristics, containing MAPK signaling pathway, Renal Cell Carcinoma, TGF-β signaling pathway, ubiquitin mediated proteolysis and Wnt signaling pathway, etc (**Figure 5k**). These results provide new clues for exploring the molecular mechanism of ccRCC in the future. In conclusion, PAEP serves as an important oncogene and is associated with a poor clinical outcome of ccRCC.

PAEP promotes proliferation, migration, and invasion of ccRCC cells

Then, we performed the transwell assays and colony formation assays to evaluate invasion, migration and proliferation in response to PAEP knockdown in 786-0 cells. Transwell assays showed that PAEP knockdown remarkably reduced cell invasion and migration in 786-0 cells, compared to Mock groups and sh Con groups ($p < 0.05$; **Figure6a, b**), Meanwhile, colony formation assays revealed that PAEP knockdown significantly reduced cell colonies in 786-0 cells compared with Mock groups and sh Con groups ($p < 0.05$; **Figure6c, d**). These results showed that PAEP participates in proliferation of 786-0 cells. Taken together, our results suggested that PAEP promoted the progression of ccRCC.

PAEP induces activation of the PI3K/Akt/NF-κ B pathway

Previous studies showed that PAEP contributed to the activation of the PI3K/Akt/NF-κ B signaling pathway. It could be inferred that PAEP played an important role in the activation of the **PI3K/Akt/NF-κ B** signaling pathway. Therefore, we performed western blotting assays to assess changed genes involved in the PI3K/Akt/NF-κ B signaling pathway in 786-0 cells. The results shown that PAEP knockdown inhibited PI3K/Akt/NF-κ B activation (**Figure7a, b**).

Discussion

In recent years, antibody immunotherapy opens new chapter for ccRCC treatment, however some people without PD-L1 expression show low objective response rates against anti-PD-L1 drugs[4, 5]. Hence, it is an urgent need to identity the novel therapeutic targets for immunotherapy. As a potential biomarker to predict immune responses, TMB had been exhibited their effect in a variety of tumor types. However, little study had focused on the relationship between the TMB and ccRCC.

In our study, we explored the status of TMB in ccRCC. The landscape of mutation profiles in TCGA-ccRCC cohort showed that 88.1% of patients develop varied types of mutation. The majority of Variant Classification, Variant Type, SNV Class were missense mutations, SNP, C>T, respectively. For the correlations between TMB and clinicopathological characteristics, the higher TMB level correlated with higher age, higher AJCC-T, grade and stage. Meanwhile, ccRCC patents with higher TMB have shorter OS. These results were in accordance with previous study[14].

Further, we identified some TMB-related immune genes through the intersection of DEGs and immune related genes, in which PAEP and LCN1 had the highest correlation. Finally, we selected the PAEP gene for the further research, which is a never reported gene in ccRCC. PAEP was overexpressed in approximately 80% of all tumors compared to normal tissue. PAEP was initially described as an immune system modulator in reproduction. Knockdown of PAEP resulted in a deregulation of immune system modulators, such as PD-L1[15, 16]. In the present study, we confirmed that PAEP was overexpressed in a cohort of 36 ccRCC patients and PAEP overexpression was closely correlated with Primary tumor size, TNM stage and Fuhrman grade. This expression pattern is similarly with the other cancers[17]. Further, PAEP is useful for determining prognosis of ccRCC and also can be severed as a potential diagnostic biomarker. PAEP

knockdown significantly inhibited the proliferation, migration and invasion of ccRCC. Our research is consistent with the function of PAEP in other cancer[15]. Mechanistically, PAEP decreased PI3K/Akt/NF-κB signaling in ccRCC. Suraj Peri have found that the NF-κB signaling is constitutively active in a high percentage of ccRCC cases[18]. Nonetheless, we found that knock down PAEP could efficiently depressed the activation of PI3K/Akt/NF-κB pathway, suggesting that PAEP maybe a potential target for this incurable malignancy.

Conclusions

In summary, our study showed that overexpression of PAEP promotes ccRCC progression may relate to the PI3K/Akt/NF-κB signaling pathway. Understanding the important role of PAEP in ccRCC would widen our knowledge of the biological basis of ccRCC progression and might represents a potential target of antibody immunotherapy for ccRCC patients.

Declarations

Ethics approval and consent to participate

All experiments were carried out in accordance with the Code of Ethics of the World Medical Association, and the study was approved by the ethics committee of Renmin Hospital of Wuhan University (approval no. 2017K-C015). All the human subjects gave their informed consent for the use of their samples and data.

Consent for publication

Not applicable.

Availability of data and materials

The datasets analyzed during the current study are available in the TCGA and Immport databases. [https://portal.gdc.cancer.gov/,https://www.immport.org/home].

Competing interests

The authors report no conflicts of interest.

Funding

NO funding.

Authors ’ contributions

Zhirong Yang and Duo Yun performed the bioinformatics analysis, drafted the manuscript and prepared the figures. Yang Su and Zhifei Che collected the clinical data. Zhifei do the experiments. Zhifei and

Yaofeng Yun design the study. Longmei Dai, Qinqin Wang, Xiangli Guo, Wang JinYong collected the related references and participated in discussion. All authors contributed to this manuscript. All authors read and approved the final manuscript.

Acknowledgments

We gratefully thank the TCGA and Immport databases for the valuable data.

References

1. Che Z, Fan J, Zhou Z, Li Q, Ma Z, Hu Z, Wu Y, Jin Y, Su Y, Liang P *et al*: **Activation-Induced Cytidine Deaminase Expression Facilitates the Malignant Phenotype and Epithelial-to-Mesenchymal Transition in Clear Cell Renal Cell Carcinoma**. *DNA Cell Biol* 2020, **39**(7):1299-1312.
2. Ljungberg B, Albiges L, Abu-Ghanem Y, Bensalah K, Dabestani S, Fernández-Pello S, Giles RH, Hofmann F, Hora M, Kuczyk MA *et al*: **European Association of Urology Guidelines on Renal Cell Carcinoma: The 2019 Update**. *Eur Urol* 2019, **75**(5):799-810.
3. Rasti A, Abolhasani M, Zanjani LS, Asgari M, Mehrazma M, Madjd Z: **Reduced expression of CXCR4, a novel renal cancer stem cell marker, is associated with high-grade renal cell carcinoma**. *J Cancer Res Clin Oncol* 2017, **143**(1):95-104.
4. Khagi Y, Kurzrock R, Patel SP: **Next generation predictive biomarkers for immune checkpoint inhibition**. *Cancer Metastasis Rev* 2017, **36**(1):179-190.
5. Nunes-Xavier CE, Angulo JC, Pulido R, López JI: **A Critical Insight into the Clinical Translation of PD-1/PD-L1 Blockade Therapy in Clear Cell Renal Cell Carcinoma**. *Curr Urol Rep* 2019, **20**(1):1.
6. Patel SP, Kurzrock R: **PD-L1 Expression as a Predictive Biomarker in Cancer Immunotherapy**. *Mol Cancer Ther* 2015, **14**(4):847-856.
7. Klempner SJ, Fabrizio D, Bane S, Reinhart M, Peoples T, Ali SM, Sokol ES, Frampton G, Schrock AB, Anhorn R *et al*: **Tumor Mutational Burden as a Predictive Biomarker for Response to Immune Checkpoint Inhibitors: A Review of Current Evidence**. *Oncologist* 2020, **25**(1):e147-e159.
8. Lee M, Samstein RM, Valero C, Chan TA, Morris LGT: **Tumor mutational burden as a predictive biomarker for checkpoint inhibitor immunotherapy**. *Hum Vaccin Immunother* 2020, **16**(1):112-115.
9. Yu G, Wang LG, Han Y, He QY: **clusterProfiler: an R package for comparing biological themes among gene clusters**. *Omics* 2012, **16**(5):284-287.
10. Robin X, Turck N, Hainard A, Tiberti N, Lisacek F, Sanchez JC, Müller M: **pROC: an open-source package for R and S+ to analyze and compare ROC curves**. *BMC Bioinformatics* 2011, **12**:77.
11. Zhang Z, Gayle AA, Wang J, Zhang H, Cardinal-Fernández P: **Comparing baseline characteristics between groups: an introduction to the CBCgrps package**. *Ann Transl Med* 2017, **5**(24):484.
12. Li H, Li Q, Ma Z, Zhou Z, Fan J, Jin Y, Wu Y, Cheng F, Liang P: **AID modulates carcinogenesis network via DNA demethylation in bladder urothelial cell carcinoma**. *Cell Death Dis* 2019, **10**(4):251.

13. Mayakonda A, Lin DC, Assenov Y, Plass C, Koeffler HP: **Maftools: efficient and comprehensive analysis of somatic variants in cancer**. *Genome Res* 2018, **28**(11):1747-1756.
14. Zhang C, Li Z, Qi F, Hu X, Luo J: **Exploration of the relationships between tumor mutation burden with immune infiltrates in clear cell renal cell carcinoma**. *Ann Transl Med* 2019, **7**(22):648.
15. Ren S, Chai L, Wang C, Li C, Ren Q, Yang L, Wang F, Qiao Z, Li W, He M *et al*: **Human malignant melanoma-derived progestagen-associated endometrial protein immunosuppresses T lymphocytes in vitro**. *PLoS One* 2015, **10**(3):e0119038.
16. Schneider MA, Granzow M, Warth A, Schnabel PA, Thomas M, Herth FJ, Dienemann H, Muley T, Meister M: **Glycodelin: A New Biomarker with Immunomodulatory Functions in Non-Small Cell Lung Cancer**. *Clin Cancer Res* 2015, **21**(15):3529-3540.
17. Ho ML, Kuo WK, Chu LJ, Yeh IH, Fan CW, Chang HI, Yuan CL, Chou TY, Chen HY, Yang SW *et al*: **N-acetylgalactosamine-6-sulfatase (GALNS), Similar to Glycodelin, Is a Potential General Biomarker for Multiple Malignancies**. *Anticancer Res* 2019, **39**(11):6317-6324.
18. Peri S, Devarajan K, Yang DH, Knudson AG, Balachandran S: **Meta-analysis identifies NF-κB as a therapeutic target in renal cancer**. *PLoS One* 2013, **8**(10):e76746.

Tables

Table 1 Correlation between PAEP expression and clinicopathologic characteristics of ccRCC patients[a]

Characteristics	N	PAEP expression level		P-value
		Low	High	
Age at surgery				0.289
<65 years	24	10	14	
≥65 years	12	8	4	
Sex				0.146
Men	25	10	15	
Women	11	8	3	
Primary tumor size				0.007
<7 cm	26	17	9	
≥7 cm	10	1	9	
pT stage				0.691
pT1-2	28	15	13	
pT3-4	8	3	5	
TNM stage				0.027
I + II	25	16	9	
III + IV	11	2	9	
Fuhrman grade				0.041
1 + 2	28	17	11	
3 + 4	8	1	7	

Abbreviations: N of cases number of cases, T stage tumor stage, TNM tumor node metastasis.

Figures

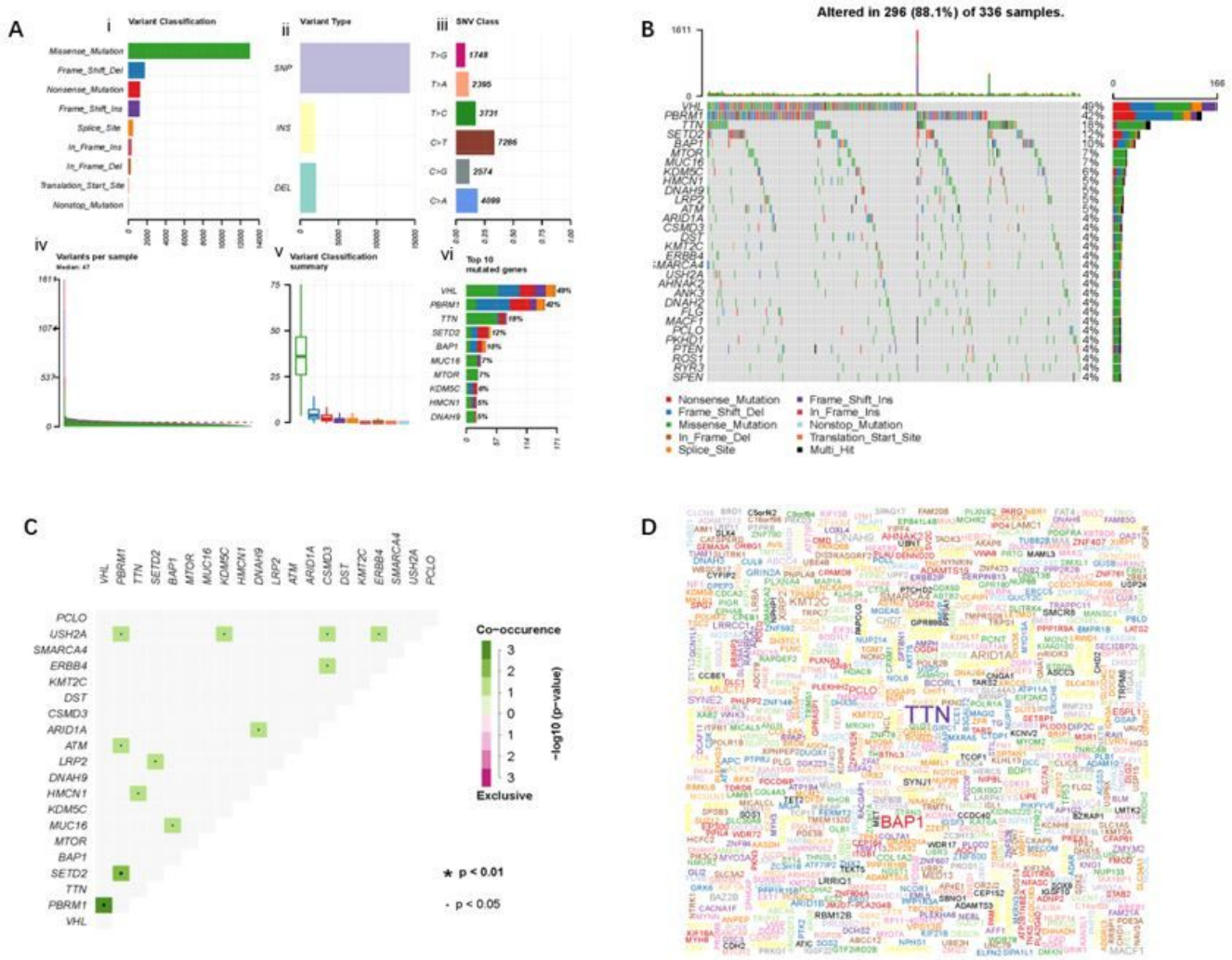

Figure 1

Landscape of gene mutations in ccRCC. (A) Landscape of mutation profiles in ccRCC cases. (a) summary of the number of variant classifications: missense mutation, frame shift del, nonsense mutation, frame shift ins, splice site, nonstop mutation, translation start site, in frame del, in frame ins; (b) counting of variant types: SNP, INS, DEL.(c) summary of base mutations: T>G, T>A, T>C, C>T, C>G and C>A. (d-e) TMB in ccRCC tissues: variants per sample and variant classification; (f) top 10 mutated genes. (B) The waterfall showed the top 10 mutated genes in ccRCC. The legend above the waterfall showed the number of altered cases in ccRCC cohort. (C) A triangular matrix showed mutually co-occurring gene pairs in ccRCC. (D) Frequency of mutated genes in ccRCC using a word cloud.

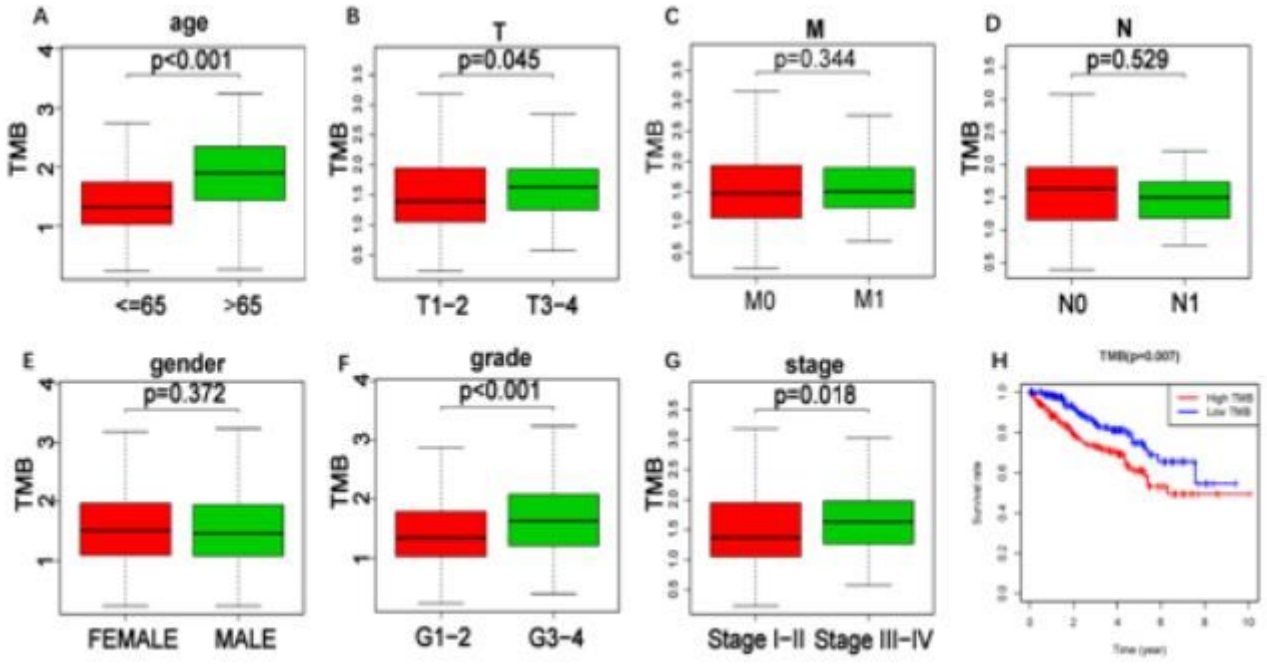

Figure 2

Correlation between TMB status and clinical characteristics of PDAC patients and prognostic value of TMB. (a-g) Lower of age and grade correlated with lower TMB level, while the gender, stage, M, N, T stage was not significant. (h) Kaplan–Meier analysis showing that higher TMB levels correlated with a poor prognosis in ccRCC patients (p<0.001). Red rectangle represents high TMB group and green rectangle represents low TMB group.

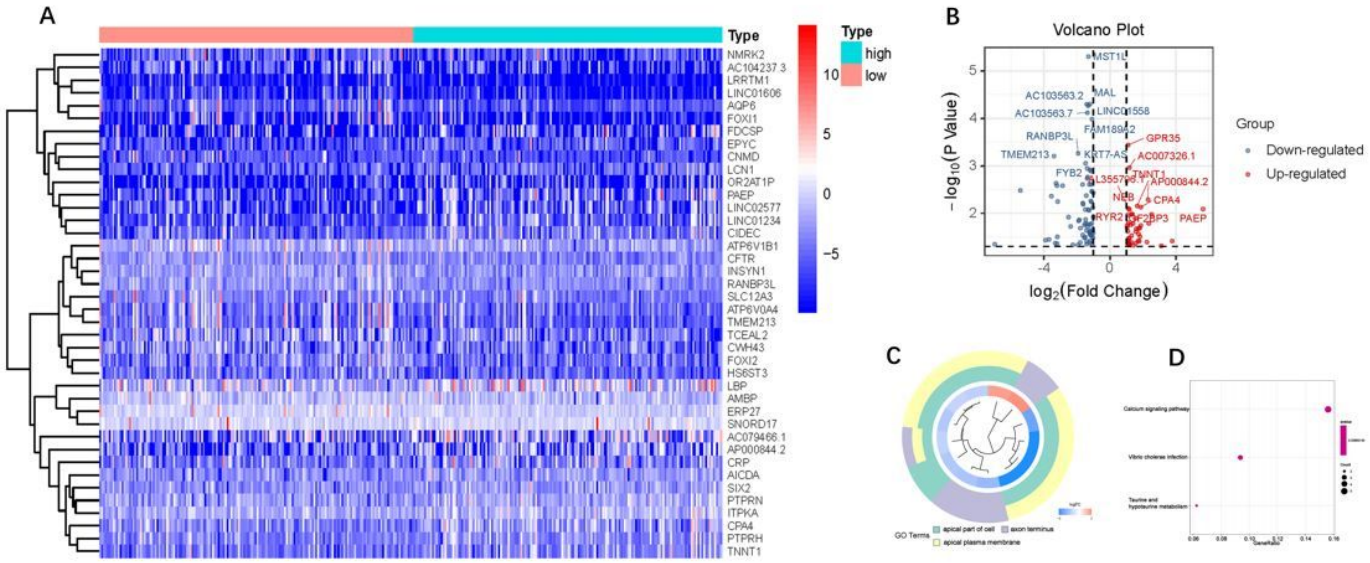

Figure 3

Differential gene expression analysis and enrichment analyses. (a) Heatmap of top 20 DEGs between high-and low-TMB groups. (b) Volcano plot of DEGs between high-and low-TMB groups. (c-d) Gene ontology and KEGG pathway enrichment analysis. DEGs were mainly enriched in immune related and cell adhesion related pathways. DEGs, differentially expressed genes.

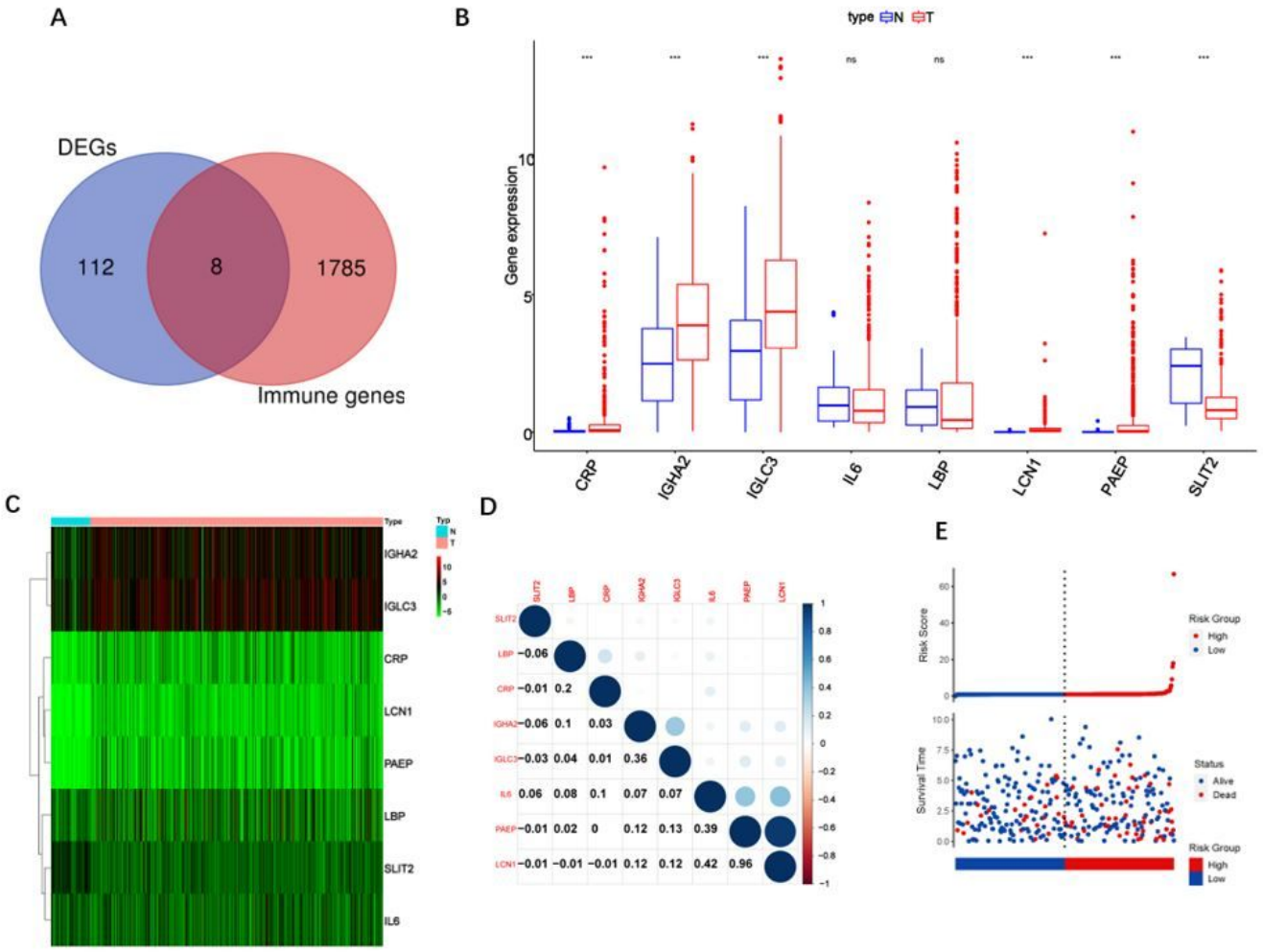

Figure 4

Identifying TMB-related immune genes and relationship of TMB-related immune genes. (a) TMB-related immune genes were identified through the intersection of DEGs and immune related genes. (b-c) Box diagram and heatmap of the expression level of all TMB-related immune genes. Most TMB-related immune genes were overexpression in tumor tissues (T), compared to normal tissues (N). *** p<0.001.(d) Correlation matrix of TMB-related immune genes. PAEP and LCN1 had the highest correlation score (0.96). (e) Distribution of risk score, survival status among patients in TCGA.TMB, tumor mutation burden; DEGs, differentially expressed genes.

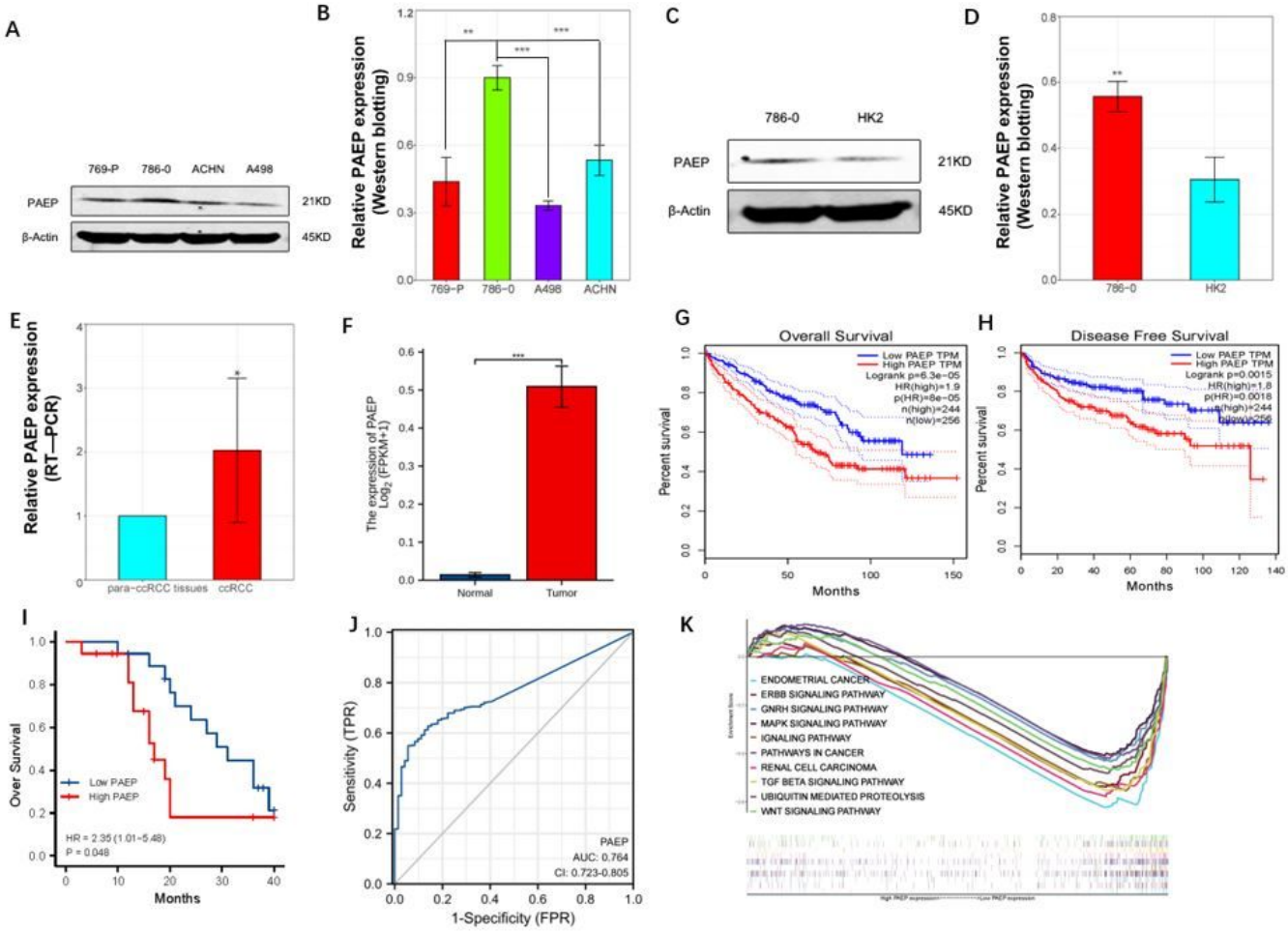

Figure 5

PAEP expression in ccRCC cells and tissues and PAEP overexpression is associated with poor prognosis of ccRCC patients. (a-b) Western blotting results and histogram analysis for the PAEP protein level in four ccRCC cell lines,769-P, 786-0, A498, ACHN. (c-d) Western blotting results and histogram analysis for the relative level of PAEP in 786-0 cells was significantly higher than that in HK2 cells. (e) RT-PCR analysis showed the expression of PAEP in human ccRCC tissues and normal adjacent tissues. (f)TCGA data showed that PAEP is upregulated in ccRCC tissues relative (n=539) to non-tumorous tissues (n=72). (g-h) ccRCC patients from the TCGA data were divided into low (n=269) and high PAEP expression groups (n=270). (i) In our cohort,the Kaplan-Meier curves showed that the ccRCC patients with high PAEP expression had shorter OS, using the median expression of PAEP as cutoff value.(j) The diagnostic value of PAEP for the ccRCC patients. (k) GSEA showed the PAEP-related pathway, including MAPK Signaling Pathway, Renal Cell Carcinoma, TGF β Signaling Pathway, Ubiquitin Mediated Proteolysis, Wnt Signaling Pathway. The experiments were independently repeated with three times (*p < 0.05, **p < 0.01, ***p < 0.001).

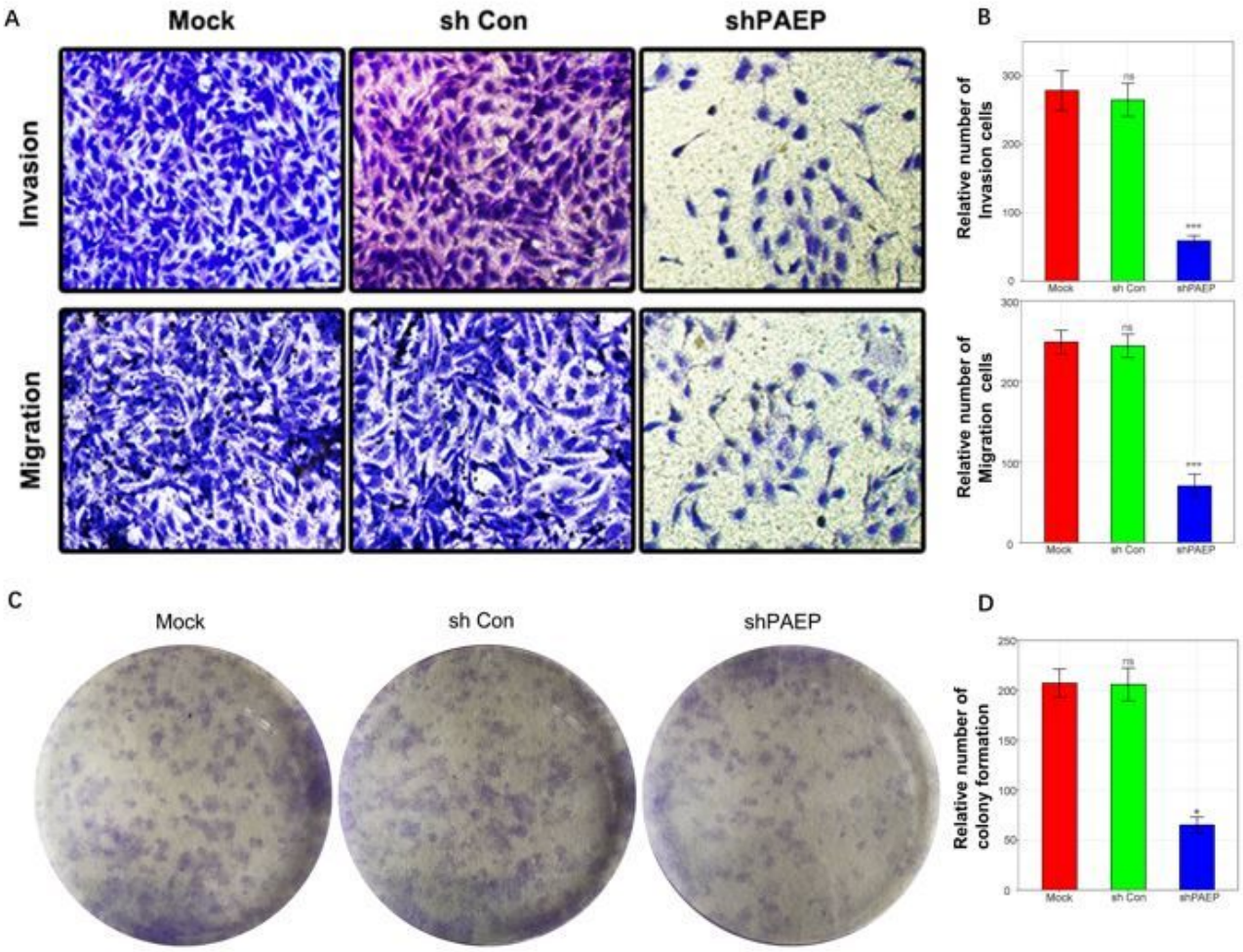

Figure 6

PAEP promotes invasion, migration, and proliferation of PDAC cells. (a-b) Representative images and histogram analysis of Transwell assays after PAEP knockdown in 786-0 cells. (c-d) Representative images and d histogram analysis of colony formation assays after PAEP knockdown in 786-0 cells. Figures with error bars show standard deviations of three independent experiments. * $p < 0.05$ and ** $p < 0.01$

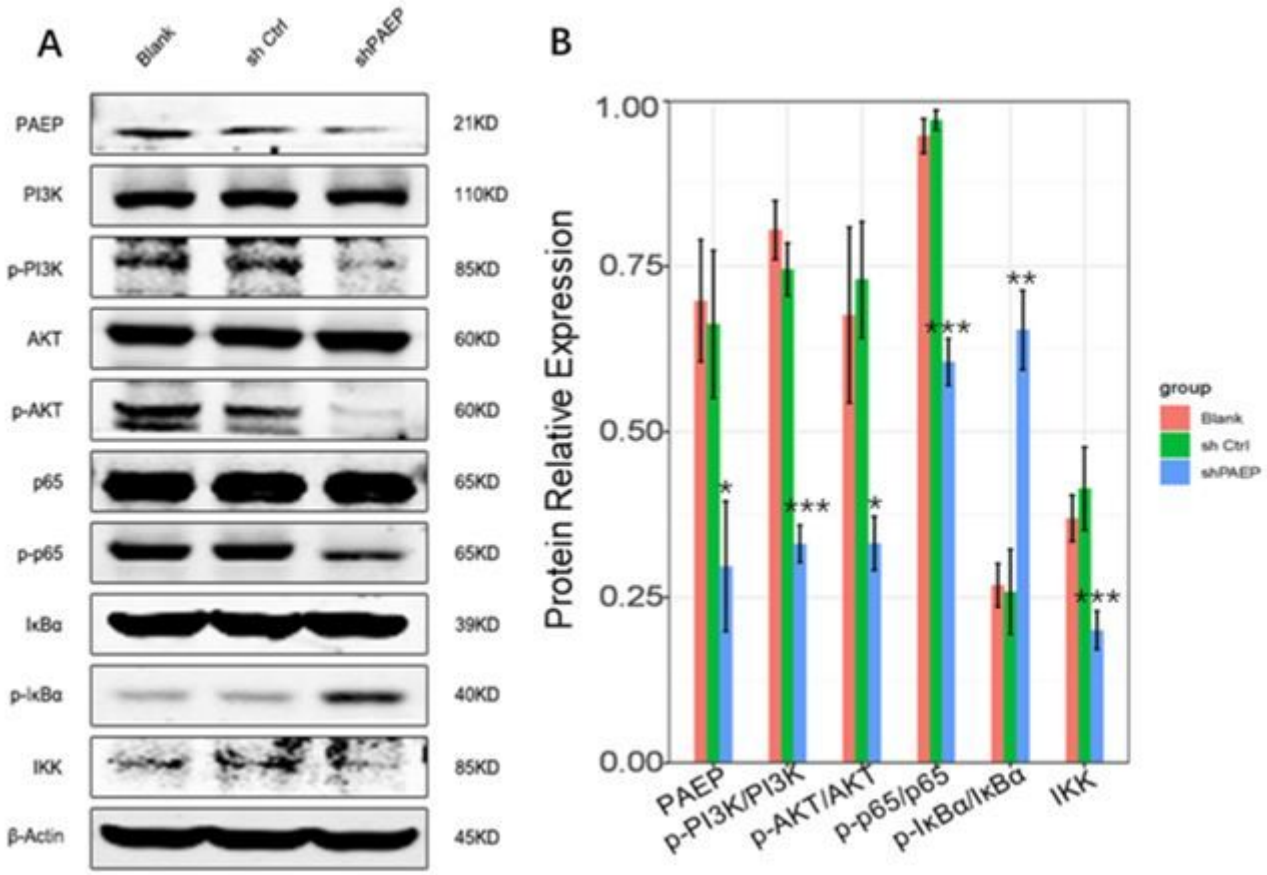

Figure 7

Effects of PAEP knockdown on PI3k-Akt-NF-Kb pathway. (a-b) Western blotting results and histogram analysis showed the changed protein levels involved in the PI3k-Akt-NF-Kb pathway after PAEP knockdown in 786-0 cells; Repression of PAEP was tested separately by Western blotting in 786-0 cells transfected with lentiviral expression vectors shRNA-PAEP and sh Ctrl. All experiments were independently repeated with three times (*p < 0.05, **p < 0.01, ***p < 0.001). shRNA, short hairpin RNA.